Korean J. Chem. Eng., 37(11), 1907-1914 (2020)
DOI: 10.1007/s11814-020-0597-z

pISSN: 0256-1115
eISSN: 1975-7220

Simultaneous removal of NO_x and SO_2 using two-stage O_3 oxidation combined with $Ca(OH)_2$ absorption

Yang Zou*,*, Yan Wang*, Xiaolong Liu*,†, Tingyu Zhu*,**,†, Mengkui Tian***, and Maoyu Cai*,***

*Beijing Engineering Research Center of Process Pollution Control, National Engineering Laboratory for Hydrometallurgical Cleaner Production Technology, Institute of Process Engineering, Chinese Academy of Sciences, Beijing 100190, China
**Center for Excellence in Regional Atmospheric Environment, Institute of Urban Environment, Chinese Academy of Sciences, Xiamen 361021, China
***School of Chemistry and Chemical Engineering, Guizhou University, Guiyang, Guizhou 550025, China
(*Received 27 November 2019 • Revised 11 May 2020 • Accepted 31 May 2020*)

Abstract−This paper proposes two-stage O_3 oxidation combined with $Ca(OH)_2$ for simultaneous removal of NO_x and SO_2 (NO_x: Nitrogen oxides including NO, NO_2 and N_2O_5). In two-stage oxidation, NO was first oxidized to NO_2 in an oxidation tube, and NO_2 was further oxidized into N_2O_5 in the spray tower. NO_x and SO_2 were simultaneously removed in the spray tower. This method can effectively reduce the extra waste of O_3 caused by the decomposition of N_2O_5, especially at high temperature. Effects of various factors on denitrification efficiency were investigated. The results showed that the NO_x removal efficiency decreased and O_3 extra consumption ratio increased with the increase of oxidation temperature or oxidation reaction time. When the O_3/NO molar ratio was 1.8, one-stage O_3 oxidation at 150 °C extra wasted 33.3% of O_3. With the increase of O_3 concentration at site 2, the NO_x removal efficiency first increased and then stabilized. Compared with the one-stage O_3 oxidation-absorption, the two-stage oxidation-absorption improved NO_x removal efficiency from 62.5% to 89%. In addition, the increase of $CaSO_3$ slurry concentration had little effect on the denitrification efficiency.

Keywords: Iron Ore Sintering Flue Gas, SO_2, NO_x, Ozone, Two-stage Oxidation

INTRODUCTION

The sintering process of iron and steel enterprises emits various air pollutants, including nitrogen oxide (NO_x), sulfur dioxide (SO_2) and particle matter (PM), which are the main precursors of the regional haze in China [1,2]. In the past decade, a series of strict environmental laws and regulations have been promulgated in China. Currently, NO_x and SO_2 control technologies for iron ore sintering flue gases can be mainly classified as flue gas desulfurization combined with selective catalytic reduction (FGD-SCR) [3-7], activated carbon technology [8-11], and ozone oxidation-absorption [12-15]. Among these technologies, ozone oxidation-absorption method has attracted much attention due to its simple structure, low operating cost, and high efficiency of SO_2 and NO_x purification.

NO accounts for more than 90% of NO_x in industrial waste gas [16], which is difficult to remove due to its more than low solubility in water. The solubility of nitrogen oxides increases with higher "N" valence states (the solubility of NO, NO_2, and N_2O_5 in water is 0.032, 213.0, and 500 g/dm^3, respectively) [17,18]. Most oxidants are effective in converting NO to NO_2, including $KMnO_4$ [19,20], Fenton's reagent [21,22], $NaClO_2$ [23,24], NaClO [25,26], EDTA [27-29], H_2O_2 [30-32], and O_3 [33-35]. However, NO_2 cannot be effectively removed by conventional absorbent [33,34,36]. Various additives have been explored to improve denitrification efficiency. $FeSO_4/CaSO_3$ [37], Fe^{3+}/H_2O_2 [38], $MgSO_4/CaSO_3$ [39], $C_6H_{15}NO_3$ (TEA)/MgO [40] and KI/Na_2CO_3 have been employed for simultaneous purification of SO_2 and NO, and the removal efficiency of SO_2 and NO was 100% and 70-95%, respectively. Nevertheless, the drawback of high consumption and high cost limits their wide applications industrially. Further oxidation of NO_2 to N_2O_5, which has the highest solubility among NO_x species [17], can greatly promote the removal of NO_x. Therefore, the deep oxidation technique has gained increasing importance.

O_3 is an efficient gas phase oxidant with high oxidation selectivity, high oxidation efficiency, fast oxidation rate and no secondary byproducts. Wang et al. [41] studied ozone oxidation combined with $Ca(OH)_2$ absorption and found that 97% of NO and nearly 100% of SO_2 were simultaneously removed. Sun et al. [33] confirmed that 87% of NO_x and nearly 100% of SO_2 could be removed using magnesia slurry combined with ozone oxidation. In addition, we studied the consumption distribution of O_3 during the oxidation-absorption process [42]. The study found that O_3 was severely wasted due to the high decomposition of N_2O_5 at high temperature. Studies have shown that the optimized temperature range of N_2O_5 formation was 80-100 °C [43,44]. When the reaction temperature is higher than this temperature range, N_2O_5 decomposes sharply and abundant O_3 will be wasted. However, iron ore sintering flue gas temperature is usually beyond 130 °C, which is not beneficial to generate N_2O_5 and will cause extra wastes of O_3 due to N_2O_5 decomposition. In the desulfurization tower, the temperature of the

†To whom correspondence should be addressed.
E-mail: liuxl@ipe.ac.cn, tyzhu@ipe.ac.cn

flue gas is commonly below 100 °C (50-60 °C for wet method and 80-90 °C for semi-dry method). If the generation of N_2O_5 is transferred into the desulfurization tower, its decomposition may be avoided.

Here in this paper, a novel method using two-stage O_3 oxidation combined with $Ca(OH)_2$ absorption is proposed. This method can effectively reduce the extra waste of O_3 caused by the decomposition of N_2O_5, especially at high temperature. The effects of O_3/NO molar ratio, oxidation temperature, oxidation reaction time, O_3 concentration injection site, SO_2 concentration and the absorbent composition on simultaneous removal of SO_2 and NO were systematically investigated.

EXPERIMENTAL SECTION

A schematic diagram of the experimental device for ozone oxidation combined with $Ca(OH)_2$ absorption is shown in Fig. 1. The device mainly included four parts: gas supply system, ozone oxidation system, wet absorption system and gas analysis system.

The simulated flue gas was provided by cylinder gases (Beijing Hua Yuan Gas Chemical Co. NO: 1%/balanced by N_2, SO_2: 2%/balanced by N_2, O_2:99.99%, N_2: 99.999%), and the flow rates were controlled by mass flow controllers (MFCs, Beijing Sevenstar Electronics Co., Ltd.). The total flow rate of simulated flue gas was 6 L/min, which was mixed in a mixing tank (diameter=10 cm, length=30 cm). Considering the NO_x and SO_2 concentrations are within the range of 150-250 ppm and 300-520 ppm in the iron ore sintering flue gas, here in this work, the initial NO and SO_2 concentration was set at 200 ppm and 500 ppm, respectively. The concentration of O_2 was 16%. Ozone was produced by Ozonia Lab2B generator using high-purity oxygen (>99.999%), which was based on the principle of high-voltage discharge. Ozone can be injected into the flue gas from two different sites (site 1 and site 2 in Fig. 1).

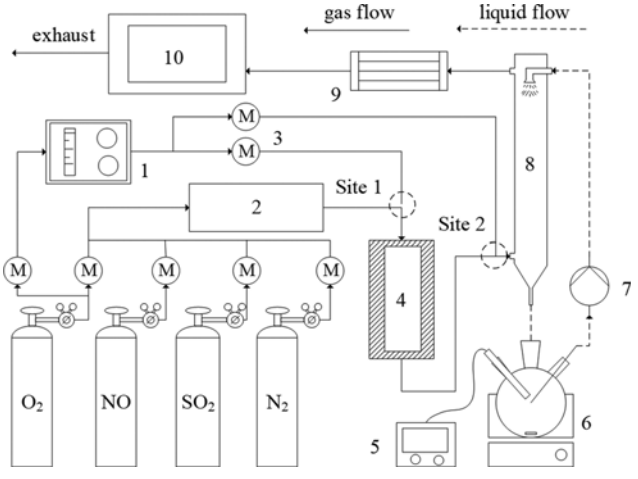

Fig. 1. Schematic diagram of the experimental apparatus.

1. Ozone generator
2. Gas mixing heating tube
3. Mass flow controllers
4. Oxidation reaction tube
5. pH meter
6. The heat-collecting magnetic heating stirrer
7. Pump
8. Spraying tower
9. Cooling device
10. Infrared gas analyzer

The flue gas residence time in the reaction tube was 1.2, 2.5 and 4.0 seconds by selecting oxidation reaction tube with different volumes. The absorption process of NO_x and SO_2 was carried out in the spaying tower with only one spray nozzle (model 1/4-1.0 mm). $Ca(OH)_2$ (99.99% w/w) and $CaSO_3$ (90% w/w) were adopted to prepare the absorbent. The absorption residence time in the spraying tower was 16 seconds. The absorbent was heated and stirred in a flask with three necks by the heat-collecting magnetic heating stirrer. Absorbent flow rate of the spray nozzle was regulated by peristaltic pump (BT100-2J, Longer Precision Pump Co., Ltd.).

A cooling device was used to remove water from the flue gas after the spraying tower. A Fourier transform infrared spectroscopy (FTIR) gas analyzer (Bruker Co., Ltd., Germany) was used to analyze the gas stream concentration (e.g. NO, NO_2, SO_2) before and after absorption.

The NO_x and SO_2 removal efficiency was calculated using Eq. (1) and Eq. (2), respectively. $[NO]_a$ and $[SO_2]_a$ are the concentrations of NO and SO_2 at the inlet of the reactor, respectively. $[NO_x]_b$ and $[SO_2]_b$ are the concentrations of NO_x and SO_2 at the outlet of the spray tower, respectively. The NO_x in this paper only includes NO, NO_2 and N_2O_5, excluding other NO_x (such as NO_3 and N_2O).

$$NO_x \text{ removal efficiency} = \frac{([NO]_a - [NO_x]_b)}{[NO]_a} \times 100\% \quad (1)$$

$$SO_2 \text{ removal efficiency} = \frac{([SO_2]_a - [SO_2]_b)}{[SO_2]_a} \times 100\% \quad (2)$$

RESULTS AND DISCUSSION

1. One-stage Oxidation-absorption

In one-stage oxidation-absorption, NO is directly oxidized into NO_2 and N_2O_5 with only one O_3 injection site. The denitrification efficiency is greatly determined by oxidation product composition. In our previous research [42], the O_3/NO molar ratio lower than 1 gave the only oxidation product as NO_2. The oxidation process was hardly affected by the oxidation temperature (60-180 °C) and the oxidation reaction time (1.2-6.7 s). When the O_3/NO molar ratio exceeded 1, the oxidation products included NO_2 and N_2O_5, and the reaction process was greatly affected by oxidation temperature and oxidation reaction time. In the range of 90-150 °C, the yield of N_2O_5 decreased with the increase of oxidation temperature or oxidation reaction time. When the O_3/NO molar ratio was 2.2, the yield of N_2O_5 was 80% (the rest was NO_2) at 90 °C. However, the yield of N_2O_5 was only 16.5% at 150 °C.

In this work, Fig. 2(a) shows the effect of oxidation temperature and O_3/NO molar ratio on the NO_x removal efficiency. It was noted that the NO_x removal efficiency increased with the improvement of O_3/NO molar ratio. For four oxidation temperatures, the NO_x removal efficiency was about 42% at an O_3/NO molar ratio of 1.0. When the O_3/NO molar ratio was greater than 1, the removal efficiency of NO_x decreased with the increase of oxidation temperature. Taking the O_3/NO molar ratio of 2.2 as an example, the removal efficiency of NO_x was nearly 100% at 90 °C, while the removal efficiency of NO_x was only 74% at 150 °C. Increase of oxidation temperature had a negative effect on NO_x removal, which is consistent

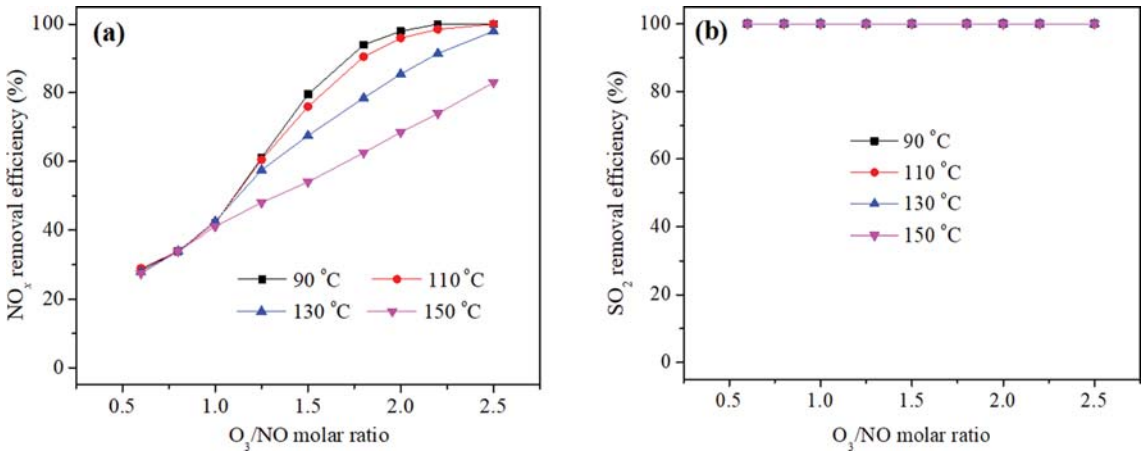

Fig. 2. Effect of oxidation temperature and O_3/NO molar ratio on the (a) NO_x removal efficiency and (b) SO_2 removal efficiency (conditions: NO, 200 ppm; SO_2, 500 ppm; O_2, 16%; $Ca(OH)_2$ slurry concentration C, 0.05 mol/L; gas flow rate Q, 6 L/min; and oxidation reaction time=1.2 s).

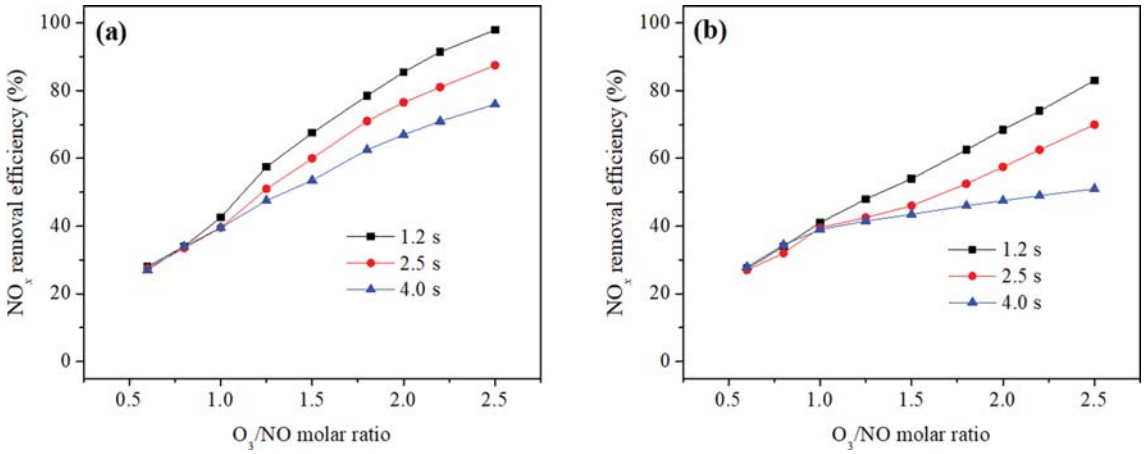

Fig. 3. NO_x removal efficiency under different O_3/NO molar ratios and oxidation reaction times at (a) oxidation temperature 130 °C and (b) oxidation temperature 150 °C (conditions: NO, 200 ppm; SO_2, 500 ppm; O_2, 16%; $Ca(OH)_2$ slurry concentration C, 0.05 mol/L; gas flow rate Q, 6 L/min).

with previous research [43]. In addition, Lin et al. [45] found that the sensitivity coefficient of the reaction changed with increasing temperature, which caused the formation of N_2O_5 to be suppressed. Therefore, the reduction in denitrification efficiency was attributed to the decrease in N_2O_5 yield. The decomposition reaction of N_2O_5 is shown in Eqs. (3) and (4).

$$N_2O_5=NO_2+NO_3 \quad (3)$$

$$2NO_3=2NO_2+O_2 \quad (4)$$

As shown in Fig. 2(b), the removal efficiency of SO_2 is nearly 100%, which was not affected by the oxidation temperature and the molar ratio of O_3/NO. It has been proved that SO_2 is difficult to oxidize into SO_3 by O_3 (Eq. (5)) in the range of 90 to 150 °C [44]. Besides, previous studies [31,33] have shown that SO_2 can be easily removed by slurry. Therefore, the oxidation temperature and O_3/NO molar ratio showed little influence on SO_2 absorption.

$$SO_2+O_3=SO_3+O_2 \quad (5)$$

Oxidation reaction time is a critical factor for the oxidation reaction. The temperature of the iron ore sintering flue gas before desulfurization is usually between 130-150 °C. Hence, the effect of oxidation reaction time on denitrification efficiency at 130 and 150 °C was investigated. Fig. 3 shows the effects of oxidation reaction time on the NO_x removal efficiency. As can be seen from Fig. 3(a) and Fig. 3(b), for three oxidation reaction times, the NO_x removal efficiency increased with the improvement of O_3/NO molar ratio. For a molar ratio of O_3/NO greater than 1, the NO_x removal efficiency decreased with the extension of oxidation reaction time. When the oxidation temperature was 130 °C and the O_3/NO molar ratio was 1.8, NO_x removal efficiency with 1.2 s, 2.5 s and 4.0 s was 78.5%, 71% and 62.5%, respectively. NO_x removal efficiency decreased with the extension of oxidation reaction time. At 130 and 150 °C, a large amount of O_3 was wasted due to the fast decomposition of N_2O_5. As the reaction time increased, N_2O_5 decomposed more, and the yield of N_2O_5 decreased. Uncreacted O_3 may still have reacted with NO_2 in the spray tower to generate N_2O_5 under low tempera-

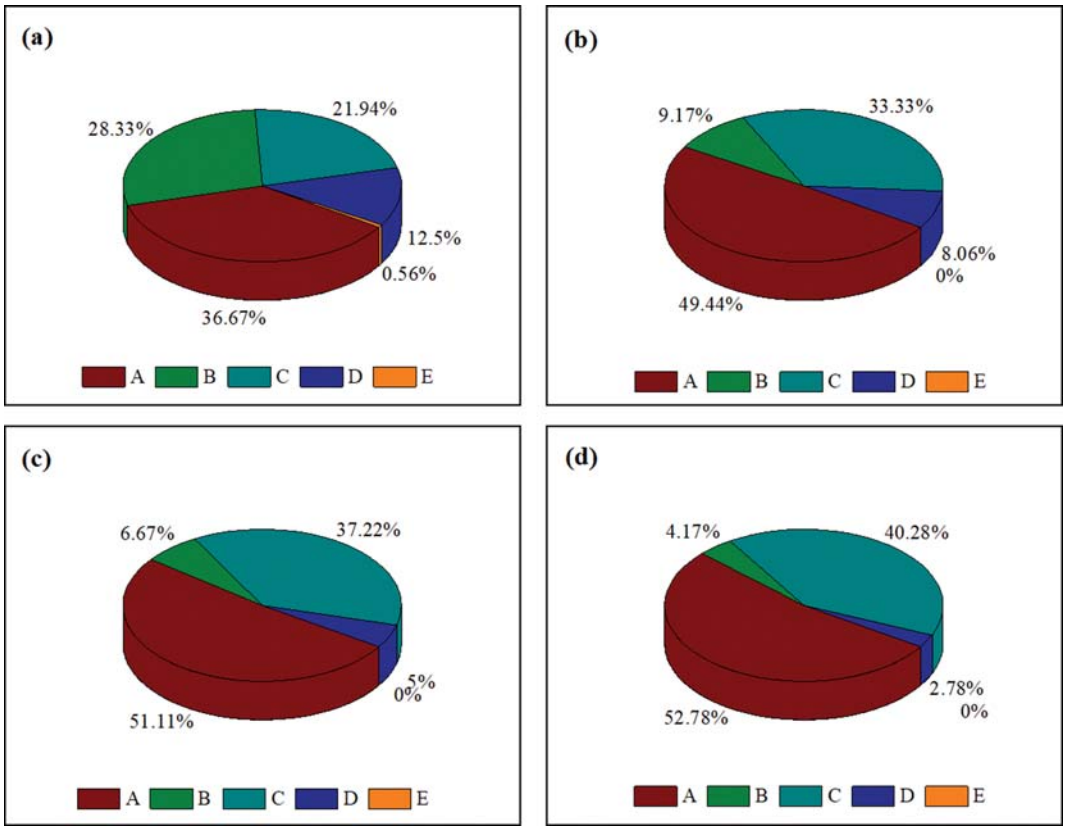

Fig. 4. Consumption distribution of O_3 in the process of $Ca(OH)_2$ combined with O_3 oxidation: (a) oxidation temperature 130 °C and oxidation reaction time 1.2 s; (b) oxidation temperature 150 °C and oxidation reaction time 1.2 s; (c) oxidation temperature 150 °C and oxidation reaction time 2.5 s; (d) oxidation temperature 150 °C and oxidation reaction time 4.0 s (conditions: NO, 200 ppm; SO_2, 500 ppm; O_2, 16%; O_3, 360 ppm; $Ca(OH)_2$ slurry concentration C, 0.05 mol/L; gas flow rate Q, 6 L/min).

tures (60 °C). However, as the oxidation reaction time increased, the O_3 entering the spray tower decreased. This indicated that a shorter oxidation reaction time was advantageous for the improvement of NO_x removal efficiency.

In our previous study [42], O_3 consumption in the oxidation-absorption process was divided into five parts. The O_3 consumption distributions under different conditions are shown in Fig. 4. (Part A: the oxidation product NO_2 corresponds to O_3 consumption; Part B: the oxidation product N_2O_5 corresponds to the O_3 consumption; Part C: some O_3 was extra wasted in invalid cyclical consumption (O_3-ICC), which was caused by N_2O_5 decomposition; Part D: the O_3 consumption in the spraying tower; Part E: the O_3 slip from the spraying tower).

As shown in Fig. 4, the ratio of Part A and Part C increased with improvement of oxidation temperature, while the ratios of Part B, Part D, and Part E decreased (the oxidation temperature of Fig. 4(a) was 130 °C; the oxidation temperature of Fig. 4(b) was 150 °C). Interestingly, as the oxidation reaction time was extended, the ratios of the various parts showed similar changing tendency (the oxidation reaction time of Fig. 4(b) was 1.2 s; the oxidation reaction time of Fig. 4(c) was 2.5 s; the oxidation reaction time of Fig. 4(d) was 4.0 s). These results indicate that increase of oxidation temperature and extension in oxidation reaction time accelerated the decomposition of N_2O_5, leading to a decrease of the N_2O_5 yield and the increase of extra waste of O_3. At an oxidation temperature of 150 °C and oxidation reaction time of 4.0 s, the additional consumption of O_3 reached a non-negligible value (40.28%). The ratio of the Part E was 0 at 150 °C, indicating that all O_3 was consumed in the oxidation-absorption process and no O_3 slip was detected.

2. Two-stage Oxidation-absorption

Based on above experiments, the denitrification efficiency for one-stage oxidation-absorption method would be ensured by lowering the oxidation temperature to 90 °C (In Fig. 2, the molar ratio of O_3/NO=2.0, and the NO_x removal efficiency was almost 100%). However, the actual flue gas temperature is not suitable to be lowered to 90 °C in the flue pipe due to the acid dew point. However, industrial flue gas contains large amounts of water and acid gases. If the flue gas temperature drops to 90 °C, the pipeline will be corroded due to water condensation.

It was found that the decrease of NO_x removal efficiency with the improvement of oxidation temperature is mainly due to the decomposition of N_2O_5. If the reaction to form N_2O_5 is transferred to the spray tower, a negative effect of high temperature on N_2O_5 may be avoided (the temperature of the flue gas in the spray tower was about 60 °C). Therefore, the two-stage oxidation-absorption was adopted for simultaneous removal of SO_2 and NO_x. A schematic diagram of the two-stage O_3 oxidation-absorption was illustrated in Fig. 5.

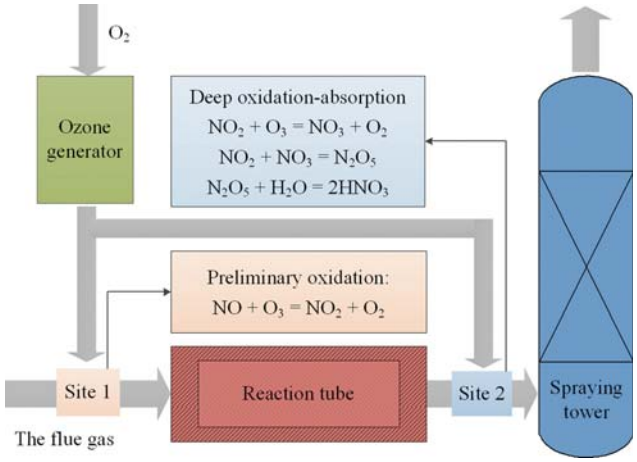

Fig. 5. Schematic diagram of two-stage O_3 oxidation-absorption.

In the two-stage oxidation-absorption method, O_3 can be better distributed in the flue gas, and O_3 slip can be prevented by adjusting the amount of O_3 at both sites. As shown in Fig. 5, NO was oxidized into NO_2 by injecting O_3 at site 1, and NO_2 was further oxidized into N_2O_5 by injecting O_3 at site 2.

The injection amount of O_3 at the two sites can be adjusted, and it is necessary to study the effect of the $[O_3]_{total}/[NO]_{total}$ molar ratio and the $[O_3]_{site1}/[NO]_{total}$ molar ratio on the NO_x removal efficiency. The NO_x removal efficiency at different $[O_3]_{total}/[NO]_{total}$ molar ratio and the $[O_3]_{site1}/[NO]_{total}$ molar ratio is shown in Fig. 6.

As shown in Fig. 6, NO_x removal efficiency increased with the increase of $[O_3]_{total}/[NO]_{total}$ molar ratio. For all molar ratios of $[O_3]_{site1}/[NO]_{total}$ greater than 1, the NO_x removal efficiency decreased as the oxidation temperature increased (the molar ratio of $[O_3]/[NO]_{total}$ remains unchanged). However, when the molar ratio of $[O_3]_{site1}/[NO]_{total}$ was less than 1, the NO_x removal efficiency did not change significantly with the change of the oxidation temperature. The main reason the oxidation temperature had a different effect on the NO_x removal efficiency was that the reaction temperature for generating N_2O_5 was different. When the molar ratio of $[O_3]_{site1}/[NO]_{total}$ was greater than 1, N_2O_5 was formed in the oxidation reaction tube, and the reaction temperature was consistent with the oxidation temperature. When the molar ratio of $[O_3]_{site1}/[NO]_{total}$ was lower than 1, N_2O_5 was formed in the spray tower, and the reaction temperature was consistent with the temperature in the spray tower and was hardly affected by the oxidation temperature.

To investigate the detailed NO_x oxidation process, experiments with two-stage O_3 oxidation without $Ca(OH)_2$ absorption were performed. The relevant oxidation data is shown in Fig. S1 and S2 (Supporting information). For the second stage oxidation, change of the molar ratio of $[O_3]_{site1}/[NO]_{total}$ had no significant effect on the yield of NO_2 and N_2O_5 at an oxidation temperature 90 °C.

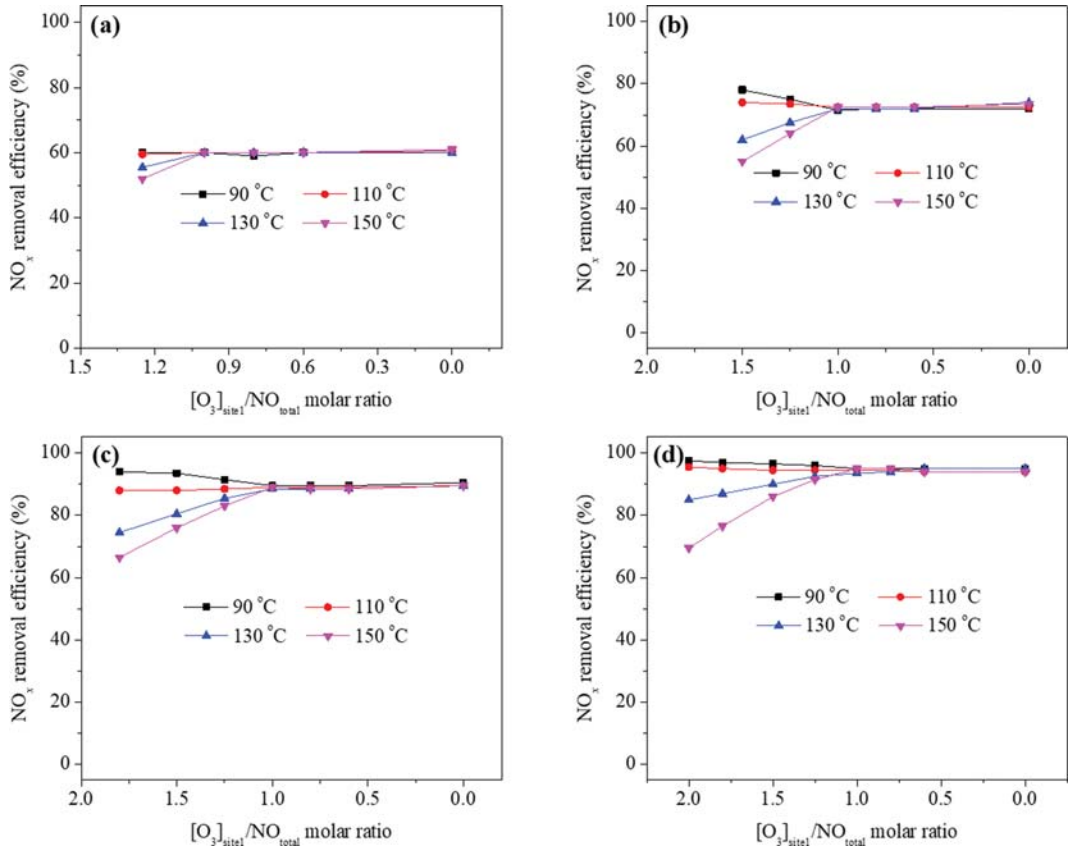

Fig. 6. NO_x removal efficiency of two-stage oxidation-absorption under different $[O_3]_{site1}/[NO]_{total}$ molar ratios. (a) $[O_3]_{total}/[NO]_{total}$=1.25; (b) $[O_3]_{total}/[NO]_{total}$=1.5; (c) $[O_3]_{total}/[NO]_{total}$=1.8; (d) $[O_3]_{total}/[NO]_{total}$=2.0. (conditions: NO, 200 ppm; SO_2, 500 ppm; O_2, 16%; $Ca(OH)_2$ slurry concentration C, 0.05 mol/L; gas flow rate Q, 6 L/min).

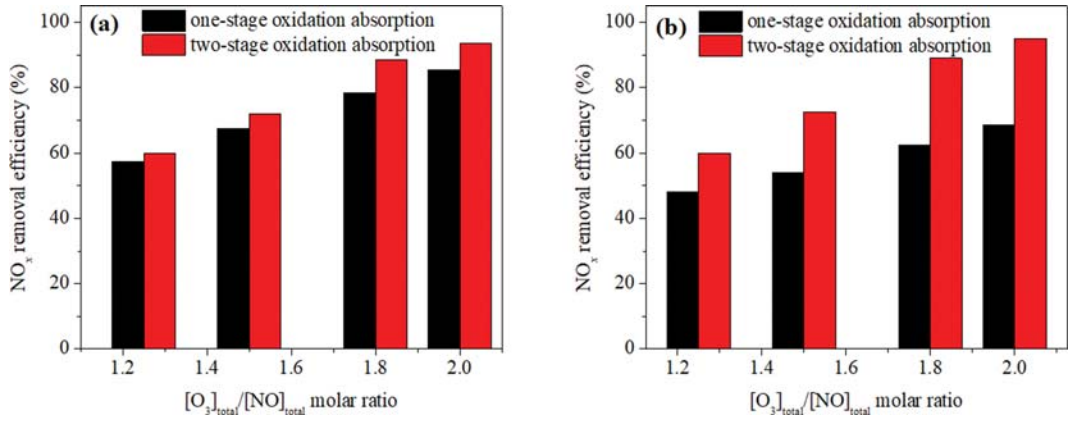

Fig. 7. Removal efficiency of NO_x by one-stage oxidation-absorption and two-stage oxidation-absorption at (a) oxidation temperature 130 °C and (b) oxidation temperature 150 °C (Conditions: NO, 200 ppm; SO_2, 500 ppm; O_2, 16%; O_3, 360 ppm; $Ca(OH)_2$ slurry concentration C, 0.05 mol/L; gas flow rate Q, 6 L/min).

When the oxidation temperature was 110, 130 and 150 °C, the NO_2 yield first decreased and then stabilized as the $[O_3]_{site1}/[NO]_{total}$ molar ratio decreased, while the N_2O_5 yield first increased and then stabilized. Increasing the yield of N_2O_5 will promote the removal of NO_x in the absorption process. Hence, it is applicable to improve the N_2O_5 yield using the two-stage oxidation method.

In addition, it was found that the NO_x removal efficiency was the highest at an oxidation temperature of 90 °C; all O_3 was injected from site 1 ($[O_3]_{site1}/[NO]_{total}=[O_3]_{total}/[NO]_{total}$). This was because N_2O_5 hardly decomposes at 90 °C. According to Chen et al. [46], NO_2^- and SO_3^{2-} were formed after NO_2 and SO_2 were absorbed by the slurry. O_3 reacts easily with them owing to its strong oxidation. If O_3 is injected at site 2, a portion of O_3 will be consumed by some side reactions, such as Eq. (6), Eq. (7) (O_3 has oxidizing properties, while SO_3^{2-} and NO_2^- have reducing properties). Although a part of the O_3 was consumed by the side reaction, O_3 slip was still detected due to the limitation of the reaction rate. The relevant data are shown in Fig. S3 (Supporting information).

$$SO_3^{2-}+O_3=SO_4^{2-}+O_2 \quad (6)$$

$$NO_2^-+O_3=NO_3^-+O_2 \quad (7)$$

From the experimental results in Fig. 6, when the $[O_3]_{total}/[NO]_{total}$ molar ratio was 1.5, 1.8 and 2.0, the NO_x removal efficiency could reach 72.5%, 89.5% and 95%, respectively. The analysis found that when the $[O_3]_{total}/[NO]_{total}$ molar ratio was 1.8, the concentration of NO_x after purification was 20 ppm, which could meet the emission requirements of iron ore sintered flue gas (Ultra-low limits for iron ore sintering process: NO_x<50 mg/Nm^3 (25 ppm)). In addition, as the $[O_3]_{total}/[NO]_{total}$ molar ratio increased, the growth rate of NO_x removal efficiency decreased ($R_{1.5\text{-}1.8}>R_{1.8\text{-}2.0}$, $R_{1.5\text{-}1.8}$ was the growth rate of NO_x removal efficiency when $[O_3]_{total}/[NO]$ molar ratio was increased from 1.5 to 1.8, $R_{1.8\text{-}2.0}$ was the growth rate of NO_x removal efficiency when $[O_3]_{total}/[NO]$ molar ratio was increased from 1.8 to 2.0). Therefore, the $[O_3]_{total}/[NO]_{total}$ molar ratio was chosen to be 1.8 in the following experiments.

The NO_x removal efficiency of one-stage oxidation-absorption and two-stage oxidation-absorption is shown in Fig. 7. The experimental results showed that the NO_x removal efficiency of the two-stage oxidation-absorption ($[O_3]_{site1}/[NO]_{total}$=1.0) was higher than that of the one-stage oxidation-absorption, especially when the oxidation temperature was 150 °C. When the oxidation temperature was 150 °C and the molar ratio of $[O_3]_{total}/[NO]_{total}$ was 1.8, the NO_x removal efficiency of the one-stage oxidation-absorption was 62.5%, and the NO_x removal efficiency of the two-stage oxidation-absorption was 89%. The main reason for the significant difference in NO_x removal efficiency was that 33.33% of O_3 in one-stage oxidation-absorption was wasted by N_2O_5 decomposition (Fig. 4(b)). These results show that two-stage oxidation-absorption was more favorable for NO_x removal when the flue gas temperature was above 130 °C.

A series of experiments with different concentrations of SO_2 and O_3 were carried out. It can be seen from Fig. 8 that the changes in the concentration of SO_2 and O_3 have a great influence on denitri-

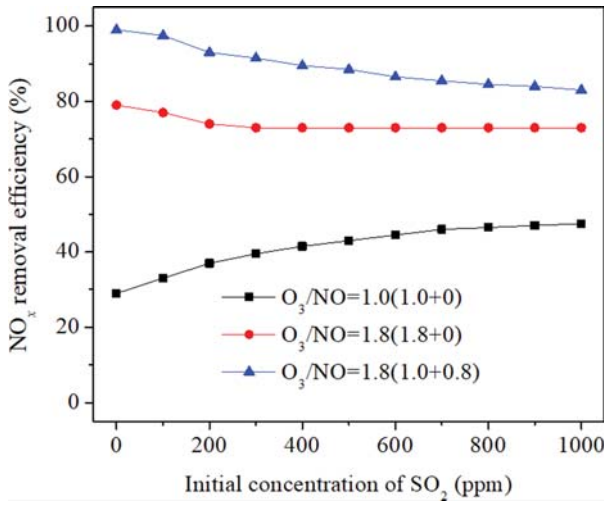

Fig. 8. Removal efficiency of NO_x under different initial concentration of SO_2 (conditions: NO, 200 ppm; SO_2, 0-1,000 ppm; O_2, 16%; O_3, 200 and 360 ppm; $Ca(OH)_2$ slurry concentration C, 0.05 mol/L; oxidation temperature T, 130 °C; gas flow rate Q, 6 L/min).

fication. When the O_3/NO molar ratio was 1, NO was oxidized to NO_2 and the denitrification efficiency increased with the increase of SO_2 concentration. It is well known that SO_2 can promote the removal of NO_2 [46,47], which can be attributed to the reaction of NO_2 with SO_3^{2-} in the slurry. However, SO_3^{2-} was produced by dissolving SO_2 in water, and its concentration increased with increasing SO_2 concentration. The reactions were as in Eqs. (8) and (9).

Note that when the O_3/NO molar ratio was 1.8, the denitrification efficiency decreased with the increase of SO_2 concentration, especially the two-stage O_3 oxidation-absorption decreased more significantly. The reason for the decrease in denitrification efficiency was that SO_3^{2-} consumes O_3 in the spray tower, reducing the formation of N_2O_5. For one-stage O_3 oxidation-absorption, N_2O_5 was mainly generated in the oxidation reaction tube, and only a small amount of O_3 entered the spray tower. For two-stage O_3 oxidation-absorption, N_2O_5 was all formed in the spray tower, and the effect of SO_3^{2-} on it was more obvious. These results indicate that the reduction in SO_2 concentration during the two-stage oxidation is favorable for the improvement of denitrification efficiency.

$$SO_2+H_2O=SO_3^{2-}+2H^+ \quad (8)$$

$$2NO_2+SO_3^{2-}+H_2O=2NO_2^-+SO_4^{2-}+2H^+ \quad (9)$$

During the desulfurization process using $Ca(OH)_2$, a certain amount of $CaSO_3$ was contained in the slurry. According to Ma et al. [34], SO_3^{2-} formed by dissolving SO_2 in water reacts with Ca^{2+} to form insoluble $CaSO_3$, as shown in Equation 10 (the solubility of $CaSO_3$ in water: 0.043 g/dm^3). Considering $CaSO_3$ is a by-product of calcium wet desulfurization, it is meaningful to investigate its influence on NO_x removal. Therefore, it is necessary to study the effect of different $CaSO_3$ concentrations on the NO_x removal efficiency of the two-stage oxidation absorption. As shown in Fig. 9, the increase in $CaSO_3$ content had no significant effect on denitrification efficiency. For the five $CaSO_3$ concentrations, as the

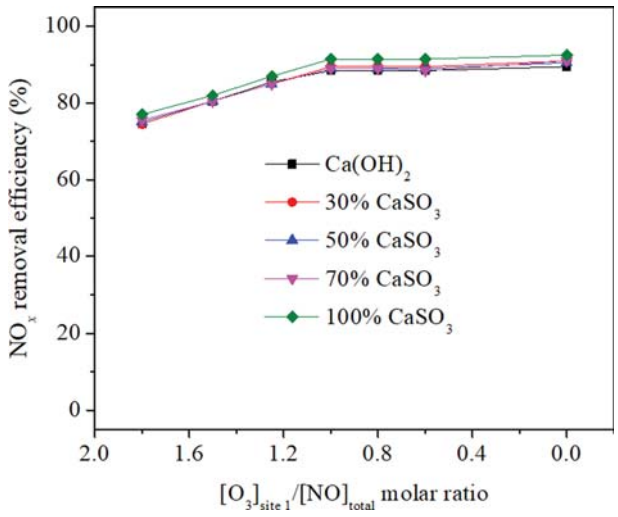

Fig. 9. Removal efficiency of NO_x under different $CaSO_3/Ca(OH)_2$ (conditions: NO, 200 ppm; SO_2, 500 ppm; O_2, 16%; O_3, 360 ppm; Calcium-based ($Ca(OH)_2$+$CaSO_3$) slurry concentration C, 0.05 mol/L; oxidation temperature T, 130 °C; gas flow rate Q, 6 L/min).

O_3 injected at site 1 decreased, the denitrification efficiency first increased and then stabilized. The solubility of $CaSO_3$ was not satisfactory. An increase in the content of $CaSO_3$ did not contribute significantly to the increase in SO_3^{2-} ion concentration. Therefore, it did not participate in the reaction related to denitrification. At the same time, it did not change the effect of O_3 injection site on denitrification efficiency. These results suggest that for two-stage oxidation $CaSO_3$ had little effect on denitrification efficiency.

$$Ca^{2+}+SO_3^{2-}=CaSO_3 \quad (10)$$

After the formation reaction of N_2O_5 was transferred to the spray tower, O_3 slip became a key concern. To avoid O_3 escape, three countermeasures are proposed: (1) Adjusting the ozone injection volume at two sites according to the temperature of the flue gas to ensure the high removal efficiency of NO_x and avoid the decomposition of N_2O_5. (2) Extension of the absorption time of the flue gas in the spray tower. (3) Adding a small amount of sulfite to increase the sulfite ion concentration in the slurry and consume the remaining O_3.

CONCLUSION

The generation of N_2O_5 was transferred to a spray tower to avoid its decomposition before spraying. The factors affecting the denitrification efficiency of O_3 oxidation combined with $Ca(OH)_2$ absorption were systematically studied. Results indicated that the optimal oxidation temperature was 90 °C, and the denitrification efficiency decreased with increasing oxidation temperature. At 130 and 150 °C, the denitrification efficiency decreased with the extension of the oxidation reaction time. A large volume of O_3 was consumed due to the decomposition of N_2O_5 at elevated temperature. When the oxidation reaction time was 1.2 s, 33.3% of O_3 was wasted at 150 °C. For the two-stage O_3 oxidation-absorption, increasing the O_3 concentration at site 2 avoided the decomposition of N_2O_5 and improved the denitrification efficiency. Compared with the one-stage oxidation-absorption, the NO_x removal efficiency of the two-stage oxidation-absorption increased from 62.5% to 89% when O_3/NO molar ratio was 1.8. Furthermore, SO_2 had a negative effect on NO_x removal when O_3 concentration was 360 ppm. Adding $CaSO_3$ to the slurry had no significant effect on denitrification efficiency. Based on these studies, three countermeasures were proposed to prevent the slip of O_3 during the two-stage O_3 oxidation-absorption process. For iron ore sintering flue gas with high temperature and low SO_2 concentration, the two-stage O_3 oxidation-absorption is advantageous for improving denitrification efficiency and reducing O_3 consumption.

ACKNOWLEDGEMENTS

This work was supported by the National key research and development program of China (2017YFC0210600) and National Natural Science Foundation of China (51978644).

ASSOCIATED CONTENT

The oxidation data of the two-stage O_3 oxidation and the O_3

slip data of the two-stage oxidation-absorption are included in the supporting information.

AUTHOR INFORMATION

Notes

The authors declare no competing financial interest.

SUPPORTING INFORMATION

Additional information as noted in the text. This information is available via the Internet at http://www.springer.com/chemistry/journal/11814.

REFERENCES

1. V. Ramanathan and Y. Feng, *Atmos. Environ.*, **43**, 37 (2009).
2. K. Li, L. Chen, S. J. White, K. Han, B. Lv, K. Bao, X. Wu, X. Gao, M. Azzi and K. Cen, *Atmos. Res.*, **192**, 38 (2017).
3. W. Chen, F. Hu, L. Qin, J. Han, B. Zhao, Y. Tu and F. Yu, *Catalysts*, **9**, 90 (2019).
4. W. Chen, Z. Li, F. Hu, L. Qin, J. Han and G. Wu, *Appl. Surf. Sci.*, **439**, 75 (2018).
5. J. Li, H. Chang, L. Ma, J. Hao and R. T. Yang, *Catal. Today*, **175**, 147 (2011).
6. J. Yu, F. Guo, Y. Wang, J. Zhu, Y. Liu, F. Su, S. Gao and G. Xu, *Appl. Catal. B-Environ.*, **95**, 160 (2010).
7. Z. Li, Y. Shen, X. Li, S. Zhu and M. Hu, *Catal. Commun.*, **82**, 55 (2016).
8. Y. Li, J.-P. Li and Z.-H. Xue, *New Carbon Mater.*, **32**, 35 (2017).
9. J. P. S. Sousa, M. F. R. Pereira and J. L. Figueiredo, *Catal. Today*, **176**, 383 (2011).
10. W. J. Zhang, S. Rabiei, A. Bagreev, M. S. Zhuang and F. Rasouli, *Appl. Catal. B-Environ.*, **83**, 63 (2008).
11. W.-J. Zhang, A. Bagreev and F. Rasouli, *Ind. Eng. Chem. Res.*, **47**, 4358 (2008).
12. W. Y. Sun, S. L. Ding, S. S. Zeng, S. J. Su and W. J. Jiang, *J. Hazard. Mater.*, **192**, 124 (2011).
13. K. Skalska, J. S. Miller and S. Ledakowicz, *Chem. Eng. Process.*, **61**, 69 (2012).
14. J. Zhang, R. Zhang, X. Chen, M. Tong, W. Kang, S. Guo, Y. Zhou and J. Lu, *Ind. Eng. Chem. Res.*, **53**, 6450 (2014).
15. K. Skalska, J. S. Miller and S. Ledakowicz, *Chem. Eng. Sci.*, **66**, 3386 (2011).
16. J. V. Durme, J. Dewulf, C. Leys and H. V. Langenhove, *Appl. Catal. B-Environ.*, **78**, 324 (2008).
17. K. Skalska, J. S. Miller and S. Ledakowicz, *Sci. Total. Environ.*, **408**, 3976 (2010).
18. Z. Han, S. Yang, X. Pan, D. Zhao, J. Yu, Y. Zhou, P. Xia, D. Zheng, Y. Song and Z. Yan, *Energy Fuels*, **31**, 3047 (2017).
19. P. Fang, C.-P. Cen, X.-M. Wang, Z.-J. Tang, Z.-X. Tang and D.-S. Chen, *Fuel Process. Technol.*, **106**, 645 (2013).
20. H. Chu, T. W. Chien and S. Y. Li, *Sci. Total Environ.*, **275**, 127 (2001).
21. Y. Zhao, R.-L. Hao, Q. Guo and Y.-N. Feng, *Fuel Process. Technol.*, **137**, 8 (2015).
22. Y. Zhao, X. Wen, T. Guo and J. Zhou, *Fuel Process. Technol.*, **128**, 54 (2014).
23. R. Hao, X. Mao, Z. Wang, Y. Zhao, T. Wang, Z. Sun, B. Yuan and Y. Li, *J. Hazard. Mater.*, **368**, 234 (2019).
24. H. W. Park, S. Choi and D. W. Park, *J. Hazard. Mater.*, **285**, 117 (2015).
25. C. V. Raghunath and M. K. Mondal, *Chem. Eng. J.*, **314**, 537 (2017).
26. C. V. Raghunath and M. K. Mondal, *Asia-Pacific. J. Chem. Eng.*, **11**, 88 (2016).
27. J. Chen, X. Zeng and Y. Deng, *Mar. Pollut. Bull.*, **113**, 87 (2016).
28. Y. G. Adewuyi and M. A. Khan, *Chem. Eng. J.*, **304**, 793 (2016).
29. Y. G. Adewuyi and M. A. Khan, *Chem. Eng. J.*, **281**, 575 (2015).
30. J. Ding, Q. Zhong, S. Zhang, F. Song and Y. Bu, *Chem. Eng. J.*, **243**, 176 (2014).
31. Y. Liu, Q. Wang, Y. Yin, J. Pan and J. Zhang, *Chem. Eng. Res. Des.*, **92**, 1907 (2014).
32. R. Hao, Y. Mao, X. Mao, Z. Wang, Y. Gong, Z. Zhang and Y. Zhao, *Chem. Eng. J.*, **365**, 282 (2019).
33. C. Sun, N. Zhao, H. Wang and Z. Wu, *Energy Fuels*, **29**, 3276 (2015).
34. Q. Ma, Z. Wang, F. Lin, M. Kuang, R. Whiddon, Y. He and J. Liu, *Energy Fuels*, **30**, 2302 (2016).
35. K. Skalska, J. Miller and S. Ledakowicz, *Chem. Pap.*, **64**, 269 (2010).
36. S. Zhou, J. Zhou, Y. Feng and Y. Zhu, *Ind. Eng. Chem. Res.*, **55**, 5825 (2016).
37. Z. Wang, X. Zhang, Z. Zhou, W.-Y. Chen, J. Zhou and K. Cen, *Energy Fuels*, **26**, 5583 (2012).
38. Y. Xing, L. Li, P. Lu, J. Cui, Q. Li, B. Yan, B. Jiang and M. Wang, *Environ. Sci. Pollut. Res.*, **25**, 6456 (2018).
39. N. Tang, Y. Liu, H. Wang, L. Xiao and Z. Wu, *Chem. Eng. J.*, **160**, 145 (2010).
40. Q. Wu, C. Sun, H. Wang, T. Wang, Y. Wang and Z. Wu, *Chem. Eng. J.*, **341**, 157 (2018).
41. Z. Wang, J. Zhou, Y. Zhu, Z. Wen, J. Liu and K. Cen, *Fuel Process. Technol.*, **88**, 817 (2007).
42. Y. Zou, X. Liu, T. Zhu, M. Tian and M. Cai, *ACS. Omega*, **4**, 21091 (2019).
43. C. Sun, N. Zhao, Z. Zhuang, H. Wang, Y. Liu, X. Weng and Z. Wu, *J. Hazard. Mater.*, **274**, 376 (2014).
44. R. Ji, J. Wang, W. Xu, X. Liu, T. Zhu, C. Yan and J. Song, *Ind. Eng. Chem. Res.*, **57**, 14440 (2018).
45. F. Lin, Z. Wang, Q. Ma, Y. He, R. Whiddon, Y. Zhu and J. Liu, *Energy Fuels*, **30**, 5101 (2016).
46. G. Chen, J. Gao, Q. Du, X. Fu, Y. Yin and Y. Qin, *Ind. Eng. Chem. Res.*, **49**, 12140 (2010).
47. D. Littlejohn, Y. Wang and S.-G. Chang, *Environ. Sel. Technol.*, **27**, 2162 (1993).

Supporting Information

Simultaneous removal of NO_x and SO_2 using two-stage O_3 oxidation combined with $Ca(OH)_2$ absorption

Yang Zou*,*, Yan Wang*, Xiaolong Liu*,†, Tingyu Zhu*,**,†, Mengkui Tian***, and Maoyu Cai*,*****

*Beijing Engineering Research Center of Process Pollution Control, National Engineering Laboratory for Hydrometallurgical Cleaner Production Technology, Institute of Process Engineering, Chinese Academy of Sciences, Beijing 100190, China
**Center for Excellence in Regional Atmospheric Environment, Institute of Urban Environment, Chinese Academy of Sciences, Xiamen 361021, China
***School of Chemistry and Chemical Engineering, Guizhou University, Guiyang, Guizhou 550025, China
(*Received 27 November 2019 • Revised 11 May 2020 • Accepted 31 May 2020*)

In order to more easily understand the removal of NO_x by two-stage O_3 oxidation-absorption, the oxidation products at two sites were studied. The first stage oxidation took place in the oxidation reaction tube, and its oxidation products were detected before site 2 and behind the oxidation reaction tube. The second stage oxidation took place in the spray tower, and its oxidation products were detected after the spray tower. It is worth noting that there was no Ca $(OH)_2$ absorption during the second stage of oxidation in the spray tower. Compared with the second stage oxidation, the two-stage oxidation-absorption reactions were more complex. Therefore, the second stage oxidation only represents the NO_x oxidation trend in the spray tower.

For the first stage oxidation, when the $[O_3]_{site1}/[NO]_{total}$ molar ratio was lower than 1, the oxidation products were composed of NO and NO_2. When the $[O_3]_{site1}/[NO]_{total}$ molar ratio was greater than 1, the oxidation products were composed of NO_2 and N_2O_5. Fig. S1 shows the relation between $[O_3]_{site1}/[NO]_{total}$ molar ratio and NO_2/N_2O_5 yield at four oxidation temperatures.

For the second stage oxidation, the NO_x oxidation process in the spray tower with four $[O_3]_{total}/[NO]_{total}$ molar ratios was studied. When $[O_3]_{total}/[NO]_{total}$ was greater than 1, the oxidation product consists of NO_2 and N_2O_5 without NO. Fig. S2 showed the relation between $[O_3]_{site1}/[NO]_{total}$ molar ratio and NO_2/N_2O_5 yield at four oxidation temperatures ($[O_3]_{site1}/[NO]_{total}$ and $[O_3]_{site2}/[NO]_{total}$ correspond to each other. When $[O_3]_{site1}/[NO]_{total}$ decreases, $[O_3]_{site2}/[NO]_{total}$ increases.)

O_3 slip is an issue that deserves attention. When the $[O_3]_{total}/[NO]_{total}$ molar ratio was 1.25 or1.5, all O_3 was consumed by the reaction in the oxidation reaction tube and spray tower, and no O_3 slip. With the increase of $[O_3]_{total}/[NO]_{total}$ molar ratio, due to the limitation of reaction rate, a small amount of O_3 did not participate in the reaction. Fig S3 showed the relation between the slip concentration of O_3 and $[O_3]_{site1}/[NO]_{total}$ molar ratio at the $[O_3]_{total}/[NO]_{total}$ molar ratio was 1.8 and 2.0.

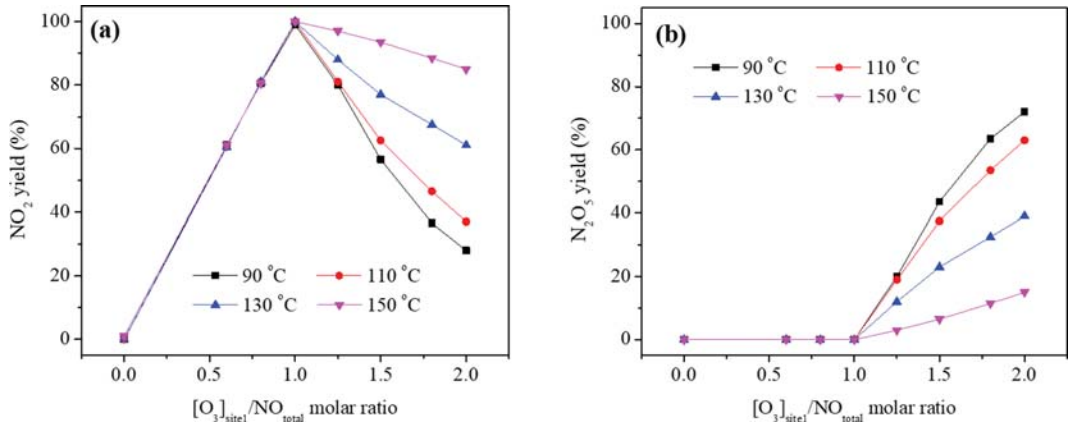

Fig. S1. NO_2/N_2O_5 yield of first stage oxidation under different $[O_3]_{site1}/[NO]_{total}$ molar ratios (conditions: NO, 200 ppm; SO_2, 500 ppm; O_2, 16%; gas flow rate Q, 6 L/min; and oxidation time=1.2 s).

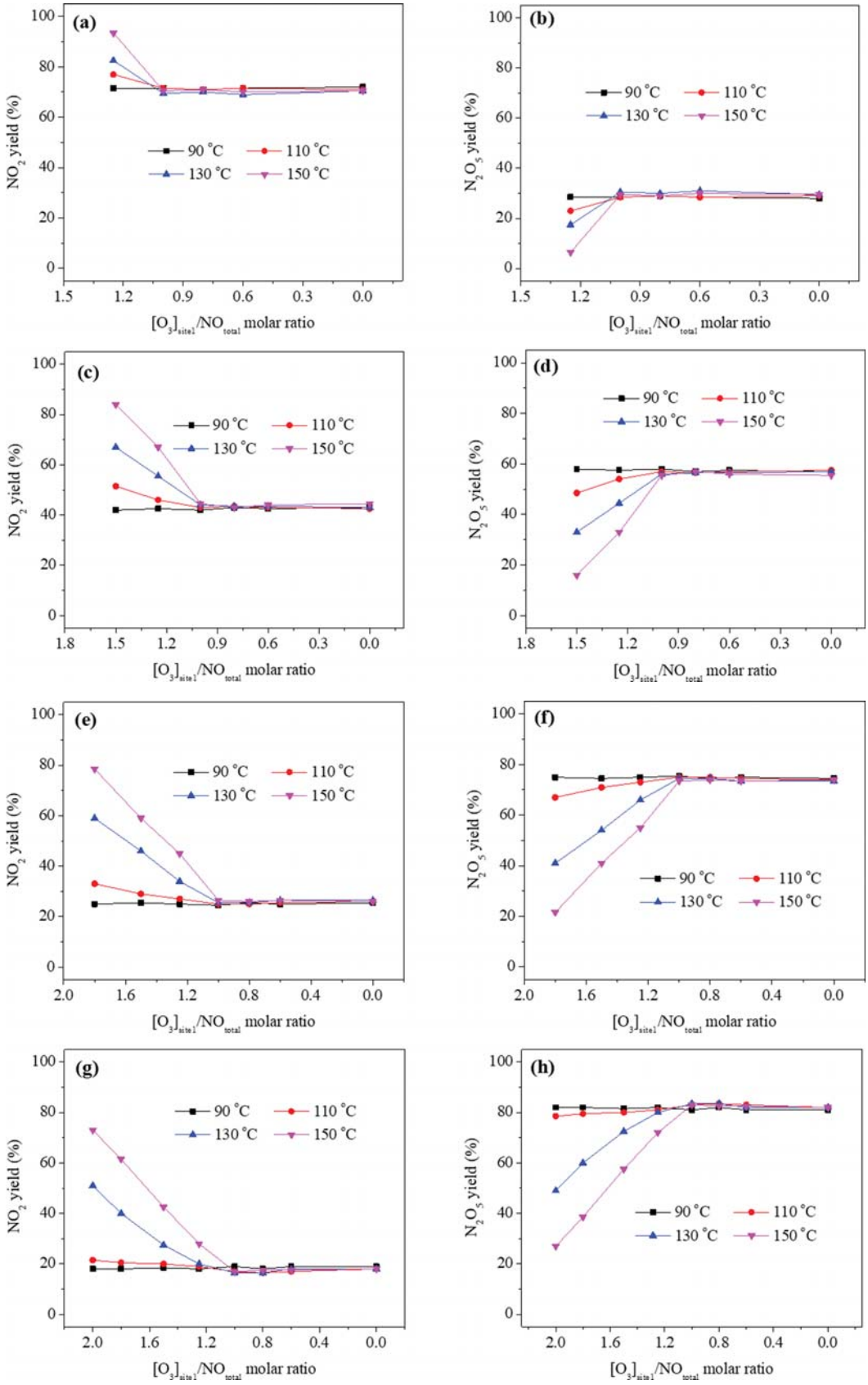

Fig. S2. NO_2/N_2O_5 yield of second stage oxidation under different $[O_3]_{site1}/[NO]_{total}$ molar ratios. (a) and (b) $[O_3]_{total}/[NO]_{total}$=1.25; (c) and (d) $[O_3]_{total}/[NO]_{total}$=1.5; (e) and (f) $[O_3]_{total}/[NO]_{total}$=1.8; (g) and (h) $[O_3]_{total}/[NO]_{total}$=2.0 (conditions: NO, 200 ppm; SO_2, 500 ppm; O_2, 16%; gas flow rate Q, 6 L/min).

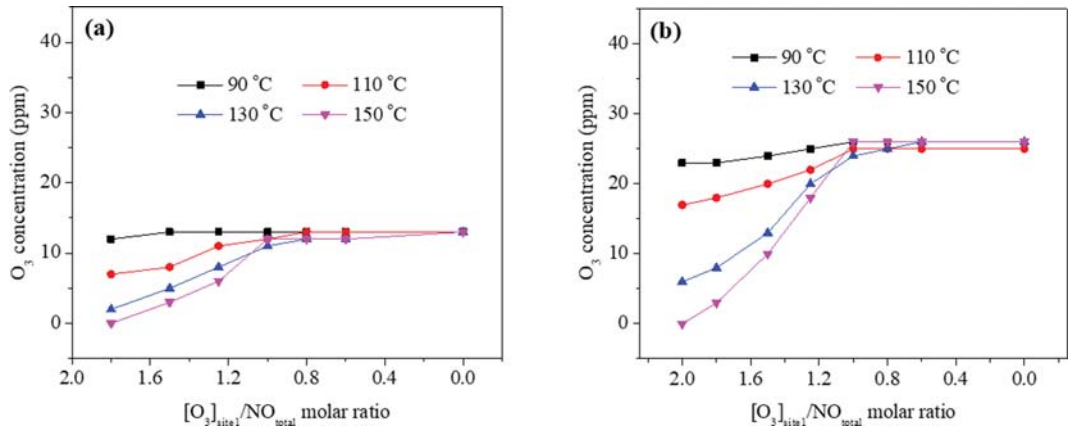

Fig. S3. O_3 slip concentration of two-stage oxidation-absorption under different $[O_3]_{site1}/[NO]_{total}$ molar ratios. (a) $[O_3]_{total}/[NO]_{total}$=1.8; (b) $[O_3]_{total}/[NO]_{total}$=2.0 (conditions: NO, 200 ppm; SO_2, 500 ppm; O_2, 16%; gas flow rate Q, 6 L/min).